Climatic Change

A simple technique for estimating an allowance for uncertain sea-level rise

John Hunter

Received: 23 June 2011 / Accepted: 20 October 2011

Abstract Projections of climate change are inherently uncertain, leading to considerable debate over suitable allowances for future changes such as sea-level rise (an 'allowance' is, in this context, the amount by which something, such as the height of coastal infrastructure, needs to be altered to cope with climate change). Words such as 'plausible' and 'high-end' abound, with little objective or statistically valid support. It is firstly shown that, in cases in which extreme events are modified by an uncertain change in the average (e.g. flooding caused by a rise in mean sea level), it is preferable to base future allowances on estimates of the expected frequency of exceedances rather than on the probability of at least one exceedance. A simple method of determining a future sea-level rise allowance is then derived, based on the projected rise in mean sea level and its uncertainty, and on the variability of present tides and storm surges ('storm tides'). The method preserves the expected frequency of flooding events under a given projection of sea-level rise. It is assumed that the statistics of storm tides relative to mean sea level are unchanged. The method is demonstrated using the *GESLA* (Global Extreme Sea-Level Analysis) data set of roughly hourly sea levels, covering 198 sites over much of the globe. Two possible projections of sea-level rise are assumed for the 21st century: one based on the Third and Fourth Assessment Reports of the Intergovernmental Panel on Climate Change and a larger one based on research since the Fourth Assessment Report.

The final publication is available at `www.springerlink.com`

Full reference: Hunter, J., 2011. A simple technique for estimating an allowance for uncertain sea-level rise, Climatic Change, DOI 10.1007/s10584-011-0332-1.

Keywords climate changes · sea-level rise · extremes

J. Hunter
Antarctic Climate & Ecosystems Cooperative Research Centre,
Private Bag 80, Hobart, Tasmania 7001, Australia
E-mail: john.hunter@utas.edu.au

1 Introduction

A major effect of climate change is a present and continuing increase in sea level, caused mainly by thermal expansion of seawater and the addition of water to the oceans from melted land ice (e.g. Meehl et al 2007, as reported in the Fourth Assessment Report (AR4) of the Intergovernmental Panel on Climate Change (IPCC)). The present rate of global-average sea-level rise is about 3.2 mm yr^{-1} (Church and White 2011). At the time of AR4 in 2007, sea level was projected to rise at a maximum rate of about 10 mm yr^{-1} and to a maximum level of about 0.8 m (relative to 1990) by the last decade of the 21st century, in the absence of significant mitigation of greenhouse-gas emissions (Meehl et al 2007, Table 10.7, including 'scale-up ice sheet discharge'). However, since the AR4, there has been considerable debate about whether these projections are underestimates (e.g. Nicholls et al (2011, Fig. 1) and Online Resource, Table (i)), as discussed in Section 5.2.

Sea-level rise, like the change of many other climate variables, will be expressed mainly as an increase in the frequency or likelihood (probability) of extreme events, rather than simply as a steady increase in an otherwise constant state. One of the most obvious adaptations to sea-level rise is to raise infrastructure by a sufficient amount so that flooding events occur no more often than they did prior to the sea-level rise. The selection of such an *allowance* has often, unfortunately, been quite subjective and qualitative, involving concepts such as 'plausible' or 'high-end' projections.

This paper develops a simple technique for estimating an allowance for sea-level rise using elementary extreme-value theory. This allowance ensures that the expected, or average, number of extreme events in a given period is conserved. In other words, any infrastructure raised by this allowance would experience the same frequency of extreme events under sea-level rise as it would without the allowance and without sea-level rise.

Present evidence (Bindoff et al 2007, Woodworth and Blackman 2004) suggests that the rise in mean sea level is generally the dominant cause of the observed increase in the frequency of extreme events (i.e. that the statistics of the effect of storminess on sea level is approximately stationary). It is therefore assumed here that there is no change in the variability of the extremes (specifically, the *scale parameter* of the Gumbel distribution; see Section 4). In other words, the statistics of storm tides relative to mean sea level are assumed to be unchanged.

The allowance derived from this method depends strongly on the probability distribution of the rise in mean sea level at some future time. However, once this distribution has been chosen, the remaining derivation of the allowance is entirely *objective*.

Unless otherwise stated, uncertainties are here given as ± one standard deviation (indicated by 'sd') or as ± the half-range (indicated by 'lim'). In the latter case, the half-range represents true limits, with zero probability outside the indicated range.

2 Statistics Which Describe the Likelihood of Extremes

Extremes are generally described by *exceedance events* which are events which occur when some variable exceeds a given level.

Two statistics are conventionally used to describe the likelihood of extreme events such as flooding from the ocean. These are the *average recurrence interval* or *ARI* (R), and the *exceedance probability* (E) for a given period (T). The ARI is the average period between extreme events (observed over a long period with many events), while the exceedance probability is the probability of at least one exceedance event happening during the period T. Exceedance distributions are often expressed (as in Section 4) in terms of the *cumulative distribution function*, F, where $F = 1 - E$. F is just the probability that there will be *no* exceedances during the prescribed period, T. These statistics are related by (e.g. Pugh 1996):

$$F = 1 - E = \exp\left(-\frac{T}{R}\right) = \exp(-N) \tag{1}$$

where N is the expected, or average, number of exceedances during the period T.

Eq. 1 involves the assumption (made throughout this paper) that exceedance events are independent; their occurrence therefore follows a Poisson distribution. This requires a further assumption about the relevant time scale of an event. If multiple closely-spaced events have a single cause (e.g. flooding events caused by one particular storm), they are generally combined into a single event using a declustering algorithm.

The occurrence of sea-level extremes, and therefore the ARI and the exceedance probability, will be modified by sea-level rise, the future of which has considerable uncertainty. For example, the projected sea-level rise for 2090-2099 relative to 1980-1999, for the A1FI Emission Scenario (which the world is broadly following at present; Le Quéré et al 2009), is 0.50±0.26 m (5%-95% range, including scaled-up ice sheet discharge; Meehl et al 2007), the range being larger than the central value.

Let us first consider a simple case in which there are two possible futures, with probabilities P_1 and P_2 ($P_1 + P_2 = 1$). If the exceedance probabilities in these two cases are E_1 and E_2, respectively, then the overall exceedance probability (taking into account both possible futures) is just $P_1E_1 + P_2E_2$. However a similar relationship does not hold for the ARI; if the respective ARIs are R_1 and R_2, then the 'overall' ARI, $P_1R_1 + P_2R_2$, has little meaning and is not useful for assessing risk. There is, nevertheless, a related variable which *may* be usefully combined probabilistically in this way - the *expected number of exceedances in a given period*.

If the period is T and the respective ARIs are R_1 and R_2, then the expected number of exceedances in each case are $N_1 = T/R_1$ and $N_2 = T/R_2$, and the overall expected number of exceedances is $P_1N_1 + P_2N_2 = T(P_1/R_1 + P_2/R_2)$.

The above can, of course be readily extended to more realistic cases in which there are more than two futures, so long as each has an estimated probability of occurrence and the sum of all the probabilities is one. There are therefore two statistical quantities which can be readily used to estimate an 'overall' result under conditions of uncertainty: the *exceedance probability*, E, and the *expected number of exceedances*, N.

If the probability distribution of the exceedance probability is given by P_E, then the overall exceedance probability, E_{ov}, is given by

$$E_{ov} = \int_{-\infty}^{\infty} P_E E \, dE \tag{2}$$

Similarly, if the probability distribution of the expected number of exceedances is given by P_N, then the overall expected number of exceedances, N_{ov}, is given by

$$N_{ov} = \int_{-\infty}^{\infty} P_N N \, dN \tag{3}$$

What are the relative merits of these two statistics? For low exceedance probabilities ($E \ll 1$), Eq. 1 indicates, using a Taylor series approximation, that $E \approx N$ (i.e. the statistics are approximately equivalent) and so the question does not arise. However, the exceedance probability is the probability of *at least* one exceedance event happening during the period T and, as E increases above about 0.6, it becomes increasingly likely that the number of events will exceed one. If the exceedance statistic is to be used to estimate *risk* (i.e. the combination of *likelihood* (E) and *consequence* (e.g. the damage cost of each event)), then knowing only the probability of *one or more events* occurring may not be sufficient – an estimate of the expected number of exceedances, N, is generally more useful.

Section 3 discusses the relationship between the exceedance probability (E) and the expected number of exceedances (N) and, in particular, the way in which this relationship is modified by additional uncertainty (yielding E_{ov} and N_{ov}).

3 The Effect of Uncertainty on a Poisson-Distributed Variable

For exceedance events that are Poisson-distributed, the relationship between E and N is given in Eq. 1 and plotted in Fig. 1 (solid curve). The solid square indicates the well-known result (e.g. Pugh 2004, p. 181) that, if the expected number of exceedances in a given period is one, then the exceedance probability is 0.63 (63%). The solid circles (*1* and *2*) indicate two possible situations (or 'futures'), as considered in the simple example of Section 2; these have exceedance probabilities $E_1 = 0.1$ (10%) and $E_2 = 0.9$ (90%), respectively. As discussed in Section 2, the overall exceedance probability and expected number of exceedances (taking into account both possible situations) are $P_1E_1 + P_2E_2$ and $P_1N_1 + P_2N_2$, respectively, where P_1 and P_2 are the respective probabilities of occurrence of situations *1* and *2*. The dashed line therefore represents the range of possible exceedance probabilities and expected numbers of exceedances for the overall outcome, for all values of P_1 and P_2 (given that $P_1 + P_2 = 1$). For example, if $P_1 = P_2 = 0.5$, then the overall values, E_{ov} and N_{ov}, are as shown by the arrow head ('ov'). The tail of the arrow indicates the expected number of exceedances for an exceedance probability of 0.5 (50%), given a Poisson distribution.

The above illustrates the general rule that, if multiple situations are considered, and if each situation is governed by a different Poisson process, then the resultant overall values (E_{ov} and N_{ov}) *do not* accord with the Poisson relationship (the continuous curve in Fig. 1). In fact, due to the curvature of the $E(N)$ relationship, the expected number of exceedances is significantly higher than the value we would

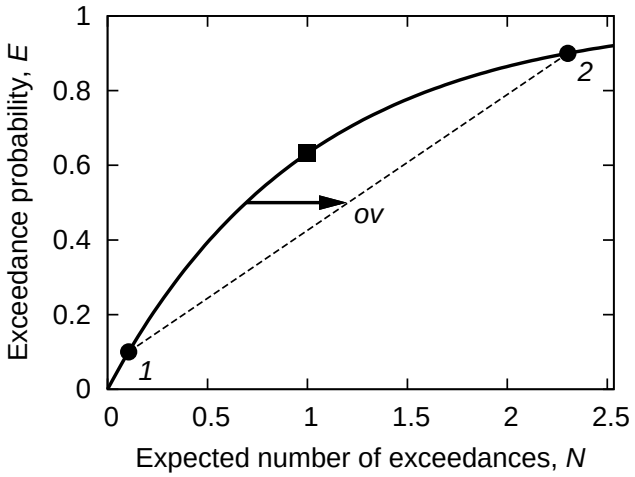

Fig. 1 Solid curve shows exceedance probability as a function of expected number of exceedances for a Poisson distribution. Solid square indicates exceedance probability of 0.63 (63%) for the case of one expected exceedance. Solid circles (*1* and *2*) indicate exceedance probabilities of 0.1 (10%) and 0.9 (90%), respectively. Dashed line represents range of possible exceedance probabilities and expected numbers of exceedances for a weighted average of values indicated by solid circles. Tail of arrow indicates exceedance probability of 0.5 (50%) for a Poisson distribution and head of arrow ('ov') indicates same exceedance probability but for simple average of values indicated by solid circles.

expect from a Poisson process with the same exceedance probability. In the present example, the overall expected number of exceedances is 1.20, compared with the 'Poisson' value of 0.69. For low exceedance probabilities, such as this, this difference is really only academic. However, if we take the case of $E_1 = 0.27$ (27%) and $E_2 = 0.99$ (99%), then (for $P_1 = P_2 = 0.5$) the overall expected number of exceedances is 2.5, compared with 1.0 for a Poisson process with the same overall exceedance probability (0.63 or 63%). It is clear from Fig. 1 that, as $E_2 \to 1$, the difference between the overall expected number of exceedances and those for a Poisson process $\to \infty$.

Planners and policymakers have had considerable experience in designing planning directives and building codes during a period of relatively unchanging climate. Let us suppose that, on the basis of previous experience, the situation for a particular item of infrastructure is presently regarded as 'safe' if the ARI (R), the exceedance probability (E) or the expected number of exceedances (N) satisfy one of the following constraints:

$$\begin{aligned} R &\geq R_{safe} \\ E &\leq E_{safe} \quad \text{for a given period, } T \\ N &\leq N_{safe} \quad \text{for a given period, } T \end{aligned} \tag{4}$$

where R_{safe}, E_{safe} and N_{safe} may be regarded as planning guidelines.

Until recently, the consideration of possible different situations (or 'futures') has not been necessary and so R_{safe}, E_{safe}, N_{safe} and T were related by Eq. 1.

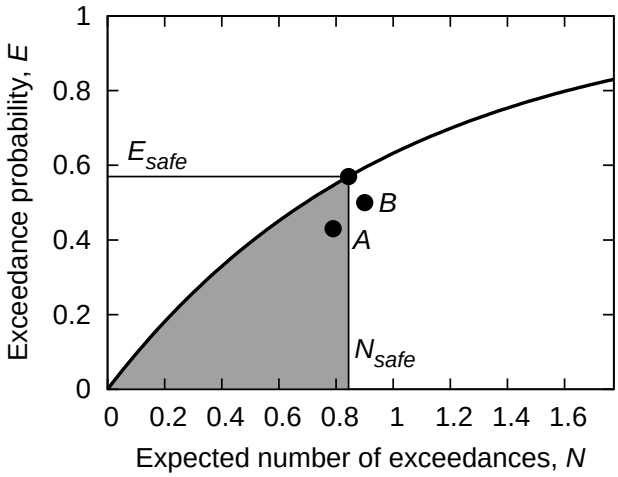

Fig. 2 Solid curve shows exceedance probability as a function of expected number of exceedances for a Poisson distribution. Solid circle (at N_{safe}, E_{safe}) represents a situation regarded as safe under conditions of relatively unchanging climate. Shaded area shows region for which $N_{ov} \leq N_{safe}$ and $E_{ov} \leq E_{safe}$ for situations (described by N_{ov}, E_{ov} in Eqs. 2 and 3) in which the uncertainty of climate change has been taken into account (requiring that they must lie *to the right of* or *below* the curve). The critical constraint is $N_{ov} \leq N_{safe}$; if this is satisfied, so also is $E_{ov} \leq E_{safe}$ (e.g. point A). However, $E_{ov} \leq E_{safe}$ does not ensure that $N_{ov} \leq N_{safe}$ (e.g. point B).

However, future climate change will bring not just *change* but also its accompanying *uncertainty*. Any new planning guidelines will therefore have to take Eqs. 2 and 3 into account, yielding estimates of E_{ov} and N_{ov}. Figure 2 indicates that, for any general future situation where the uncertainty of climate change has been taken into account, the critical constraint is $N_{ov} \leq N_{safe}$; if this is satisfied, so also is $E_{ov} \leq E_{safe}$ (e.g. point A). However, $E_{ov} \leq E_{safe}$ does not ensure that $N_{ov} \leq N_{safe}$ (e.g. point B).

It is therefore concluded that future allowances for climate change extremes (e.g. related to sea-level rise) should be based on estimates of the *expected number of exceedances* rather than on the *exceedance probability*. Section 4 now describes the derivation of an allowance for uncertain sea-level rise which conserves the expected number of exceedances in a given period.

4 Theory

The probability of exceedances above a given level and over a given period is often well described by a *generalised extreme-value distribution (GEV)*. The simplest of these, the *Gumbel* distribution, fits most sea-level extremes quite well (e.g. van den Brink and Können 2011). The Gumbel distribution may be expressed as (e.g. Coles 2001, p. 47)

$$F = \exp\left(-\exp\left(\frac{\mu - z}{\lambda}\right)\right) \tag{5}$$

where z is the height, μ is the 'location parameter' and λ is the 'scale parameter' (an e-folding distance in the vertical). F is the probability that there will be no exceedances $> z$ during the prescribed period, T.

From Eqs. 1 and 5

$$N = \exp\left(\frac{\mu - z}{\lambda}\right) \tag{6}$$

μ is therefore the value of z for which $N = 1$ during the period T.

As noted in Section 1, it is assumed that the scale parameter, λ, does not change with a rise in sea level.

Given that the scale parameter is a key player in the present work, it is worth considering the factors which determine its magnitude. Firstly, the scale parameter relates to *extremes* and therefore to the variability of the *maxima* in sea level (over some prescribed period such as a year), rather than to the *total* variability in sea level. Therefore a *large* tidal range, with only *weak* modulation (i.e. almost a pure sinusoid) would have a *small* scale parameter. Conversely, a *small* tidal range, with *strong* modulation (e.g. a strong neap/spring cycle) would have a *large* scale parameter. The situation is further complicated by the character of the storm surges, so that *tidal range* is not a good indicator of the magnitude of the scale parameter. For example, in Australia, the tidal range at Sydney (1.3 m) is over twice the range at Fremantle (0.6 m). However, the scale parameter at Sydney (0.06 m) is only half of the scale parameter at Fremantle (0.12 m).

Mean sea level is now raised by an amount $\Delta z + z'$, where Δz is the central value of the estimated rise and z' is a random variable with zero mean and a distribution function, $P(z')$, to be chosen below. This effectively increases the location parameter, μ, by $\Delta z + z'$. From Eqs. 3 and 6, the expected number (N_{ov}) of exceedances ($> z$) during the period T, now becomes

$$\begin{aligned} N_{ov} &= \int_{-\infty}^{\infty} P(z') \exp\left(\frac{\mu - z + \Delta z + z'}{\lambda}\right) dz' \\ &= N \exp\left(\left(\Delta z + \lambda \ln\left(\int_{-\infty}^{\infty} P(z') \exp\left(\frac{z'}{\lambda}\right) dz'\right)\right) \Big/ \lambda\right) \end{aligned} \tag{7}$$

(noting that we again use the subscript 'ov' to indicate integration over a range of possibilities).

The term $\lambda \ln(\cdots)$ in the last part of Eq. 7 represents an *additional* allowance arising from the *uncertainty* in future sea-level rise. It is evaluated for three types of distribution: a normal distribution, a boxcar (uniform) distribution and a raised cosine distribution (see Online Resource, Section A). The resulting allowances are all expressed as simple analytical expressions, involving the Gumbel scale parameter, λ, the central value of the estimated rise, Δz, and its standard deviation, σ. The boxcar and raised cosine distributions, which have upper and lower limits, are considered here because there are quite strong physical constraints on sea-level rise. For example, it is highly unlikely that sea level will fall under global warming and Pfeffer et al (2008) deduced an upper limit of sea-level rise for the 21st century of 2.0 m. The raised cosine distribution (which is used later to describe a possible 21st-century sea-level rise projection) is given by:

$$P(z') = \frac{1}{W}\left(1 + \cos\left(\frac{2\pi z'}{W}\right)\right) \quad \text{for} \quad -W/2 < z' < W/2 \quad \text{otherwise} \quad 0 \qquad (8)$$

where W is the full-width of the distribution.

5 Projections of Sea-Level Rise

The sea-level rise allowance described in Section 4 requires an estimate of the mean sea-level rise, Δz, and its uncertainty, σ. These estimates may be provided by combining results from the IPCC Assessment Reports (specifically, the Third Assessment Report (TAR; Church et al 2001) and the AR4 (Meehl et al 2007)), and from research conducted since the AR4, as summarised for example by Nicholls et al (2011). As will be seen, these two sources of information (i.e. TAR/AR4 and post-AR4) lead to two rather distinct ranges and are treated separately in the following discussion. At present, it is unclear which of the two is the more appropriate.

It should also be noted that there is considerable disagreement between models as to the regional variation of future sea-level rise (Meehl et al 2007, Figure 10.32). The present work uses only projections of *global-average* sea-level rise; regional variation therefore represents additional uncertainty.

The projections described here apply only to the component of sea-level rise that is related to anthropogenic climate change. They do not include any effects of vertical land movement, such as those associated with glacial isostatic adjustment, tectonic activity or local land sinkage (e.g. due to groundwater withdrawal). Any such movement, and its uncertainty, should be incorporated into the projections, to yield the sea-level rise relative to the land.

5.1 The TAR and AR4 Projections

For each of the six 'marker' emission scenarios (A1B, A1T, A1FI, A2, B1 and B2), the TAR gave the 'range of all AOGCMs *(Atmosphere-Ocean General Circulation Models)* ... including uncertainty in land-ice changes, permafrost changes and sediment deposition' at decadal increments through the 21st century, relative to 1990 (Church et al 2001, Table II.5.1). The 'range of all AOGCMs' has been interpreted to be ± 2 standard deviations (Church et al 2001, Box 11.1; Meehl et al 2007, 10.A.6). On the other hand, the AR4 gave the '5 to 95% range (m) of the rise in sea level' and included an additional contribution ('scaled-up ice sheet discharge') to account for 'rapid dynamical changes' in ice sheets that were not simulated by continental ice sheet models (Meehl et al 2007). The AR4 results were only presented as the sea-level rise for 2090-2099 relative to 1980-1999. Both the TAR and AR4 results apparently relate to the *spread* of model projections (akin to the *standard deviation*) rather than to the uncertainty (akin to the *standard error*) of the best estimate of the projections. The uncertainty, σ, used in Section 4 and in Online Resource, Section A, Eqs. (viii), (ix) and (x), strictly relates to the *standard error*. However, for reasons discussed in Online Resource, Section B, the

uncertainty, σ, is here associated with the *standard deviation* (rather than the *standard error*) of the projections.

In order to obtain time series of model projections through the 21st century that are compatible with the AR4, Hunter (2010) fitted the time series of TAR projections through the AR4 projections for 2090-2099. The resultant tables (Hunter 2010, Tables 1 and 2) are similar to Table II.5.1 of the TAR, except that they relate to the 5 to 95% range, rather than to the 'range of all AOGCMs'. They are here referred to as the *AR4-adjusted TAR projections*. It should be noted that, for the last decade of the 21st century, these *are* the AR4 projections.

Therefore, the first set of sea-level rise allowances is based on the A1FI emission scenario (which the world is broadly following at present; Le Quéré et al 2009) and the *AR4-adjusted TAR projections*, as follows:

1. the mean sea-level rise, Δz, was derived from the average of the 5 and 95% values, and
2. the uncertainty, σ, was approximated by the *standard deviation* of the projections, assuming a normal distribution fitted through the 5 and 95% values.

This is here denoted the *IPCC A1FI Projection*.

5.2 Post-AR4 Projections

Prior to the publication of the AR4, Rahmstorf et al (2007) compared the projections of the TAR with observations from 1990 to 2006 and concluded that the observations were following the 'model maximum' projections, which are about 70% greater than the central value of the projections. Further, the present observed rate since 1993 (3.2 mm yr^{-1}, Church and White 2011) is about 60% greater than the central value of sea-level rise from 1990 to 2010 (about 2.0 mm yr^{-1}), derived from the *AR4-adjusted TAR projections* (see Section 5.1 and Hunter (2010)). However, simple comparisons between the projected and observed sea-level rise over the past two decades should be treated with some caution for two main reasons:

1. The comparison may be confounded by interannual and decadal variability. For example, Church and White (2011) showed that the satellite altimeter observations started (in 1993) during a period of relatively low sea level following (and possibly forced by) the Mt Pinatubo eruption in 1991; allowance for this relative low in observed sea level reduces the disagreement between observations and projections for 1990-2010 from 60% to about 45% (with the observations still being larger than the projections).
2. There is no obvious physical reason why any present proportional relationship between observations and projections should be maintained until the end of the century.

Nicholls et al (2011) summarised projections of sea-level rise published since the AR4 (Online Resource, Table (i) and their Fig. 1). They suggested 'a pragmatic range of 0.5-2 m for twenty-first century sea-level rise, assuming a 4° C or more rise in temperature'. This temperature rise (which is for 2090-2099 relative to 1980-1999), is achieved by the AR4 temperature projections for emission scenarios A1B, A2 and A1FI. They also concluded that 'the upper part of this range is considered

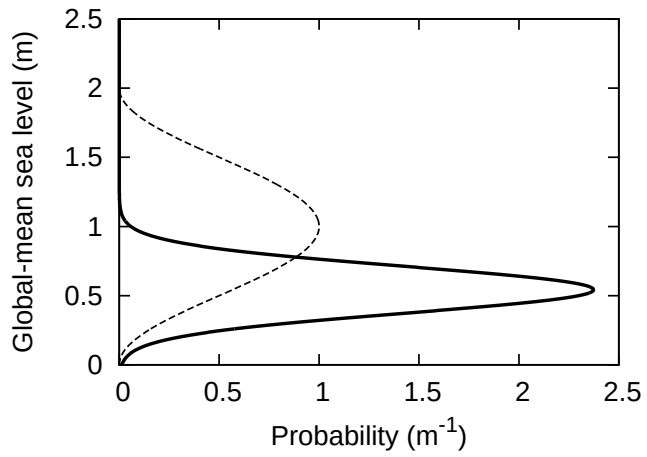

Fig. 3 Probability distributions for global-average rise in mean sea level. Solid curve shows *IPCC A1FI Projection* for 1990-2100, based on A1FI emission scenario and *AR4-adjusted TAR projections* (normal distribution with $\Delta z = 0.542$ m and $\sigma = 0.168$ m). Dashed curve shows *1.0/1.0 m Projection* for the 21st century, based on post-AR4 results (raised cosine with $\Delta z = 1.0$ m and $W/2 = 1.0$ m).

unlikely to be realized' (the 2 m upper limit of this range being derived from Pfeffer et al (2008)). It is also highly unlikely that sea level will fall under global warming. These considerations are here translated into a 21st century sea-level rise of 1.0 m $\pm$ 1.0 (lim) m, using a raised-cosine probability distribution giving zero probability outside this range (Eq. 8). The second set of sea-level rise allowances is provided, based on this projection, which is here denoted the *1.0/1.0 m Projection*.

5.3 Summary of Projections

Two sets of allowances are therefore provided for 2100:

1. the *IPCC A1FI Projection* for 2100 relative to 1990, which is based on the A1FI emission scenario and the *AR4-adjusted TAR projections* (Hunter 2010), giving $\Delta z = 0.542$ m and $\sigma = 0.168$ m (normal distribution), and
2. the *1.0/1.0 m Projection* for the 21st century, which is based on post-AR4 results (Nicholls et al 2011), giving $\Delta z = 1.0$ m and $W/2 = 1.0$ m (raised cosine distribution, Eq. 8). The standard deviation of this projection is 0.362 m (see Online Resource, Section A), so that the *1.0/1.0 m Projection* is roughly twice as large in both mean and standard deviation as the *IPCC A1FI Projection*.

These probability distributions are shown in Fig. 3. Given the present uncertainties in the processes which determine sea-level rise, it is difficult to assign meaningful weights to these two projections. However, it should be noted from Section 5.2 that the present observations of sea-level rise lie roughly mid-way between the two projections.

6 Application of the Method

6.1 Introduction

The scale parameter (λ) was estimated from the *GESLA* (Global Extreme Sea-Level Analysis) sea-level database (see Menéndez and Woodworth 2010) which has been collected through a collaborative activity of the Antarctic Climate & Ecosystems Cooperative Research Centre, Australia, and the National Oceanography Centre Liverpool (NOCL), UK. The data covers a large portion of the world and is sampled at least hourly (except where there are data gaps). The database was downloaded from NOCL on 26 October 2010 and contains 675 files. However, many of these files are near-duplicates provided by different agencies. Many are also as short as one or two years and are therefore not suitable for the analysis of extremes. Initial data processing was therefore performed as described in Online Resource, Section C.

Prior to extremes analysis, the data were 'binned', so as to produce files with a minimum sampling interval of one hour, and detrended. Annual maxima were estimated using a declustering algorithm such that any extreme events closer than 3 days were counted as a single event, and any gaps in time were removed from the record. These annual maxima were then fitted to a Gumbel distribution using the *ismev* package (Coles 2001, p. 48) implemented in the statistical language *R* (R Development Core Team 2008). This yielded the scale parameter (λ) for each of the 198 records. It is assumed that λ does not change in time.

The results are here presented in three different ways. Firstly, the scale parameter indicates the way in which the frequency of extreme events changes for a given rise in mean sea level. From Eq. 6, a rise of mean sea level, δz, (which effectively increases the location parameter, μ, by δz) increases the expected number of exceedances, N, by a factor $\exp(\delta z/\lambda)$. This factor is shown (using the *left-hand key* in the figures) for a rise in mean sea level of 0.5 metres in Fig. 4 (for the world) and in Online Resource, Fig. (i) (for Australia).

The other, and closely related, way of presenting the results is in terms of the sea-level rise allowances for a normal uncertainty distribution (Online Resource, Section A, Eq. (viii)) and for a raised-cosine uncertainty distribution (Online Resource, Section A, Eq. (x)). Since all three ways of presenting the results depend spatially only on the scale parameter, λ, they are here plotted in the same figures, but with different keys (the allowances being shown by the *middle* and *right-hand keys*).

The results are also summarised for a number of specific locations in Online Resource, Table (ii).

6.2 Multiplying Factor for 0.5 m Sea-Level Rise

Fig. 4 shows significant global variability of the Gumbel scale parameter, and hence in the increase in frequency of flooding events for a given sea-level rise (*left-hand key*). The largest values of this multiplying factor are in the southern Caribbean Sea (Cristóbal and Cartagena) while the smallest lie along the Pacific coast of Alaska, Canada and the northwest USA; in the mid-east coast of the USA; and around the northwest European shelf and the Baltic. The *large* values

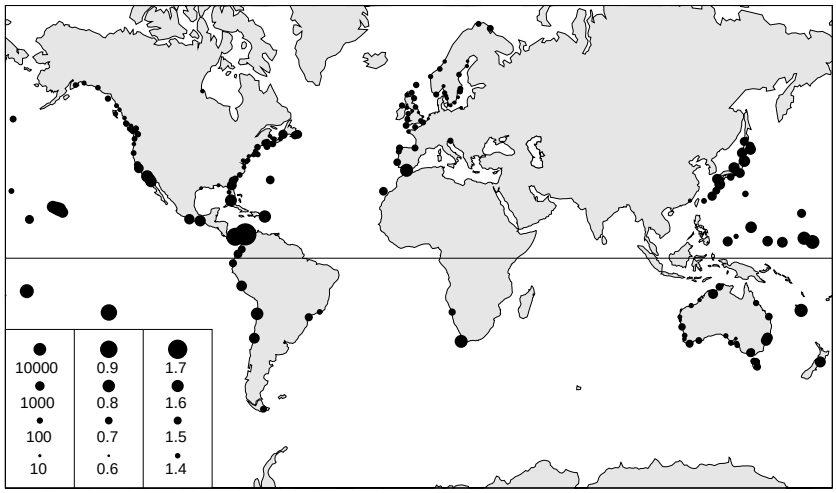

Fig. 4 Results of global analysis, indicated by dot diameter. (a) Factor by which frequency of flooding events will increase with a rise in sea level of 0.5 metres (key is left-hand column of dots in the bottom left-hand corner). (b) Sea-level rise allowance (metres) for 1990-2100 which conserves frequency of flooding events for the *IPCC A1FI Projection* based on A1FI emission scenario and *AR4-adjusted TAR projections* (normal distribution with $\Delta z = 0.542$ m and $\sigma = 0.168$ m); key is central column of dots in the bottom left-hand corner. (c) Sea-level rise allowance (metres) for 21st century which conserves frequency of flooding events for the *1.0/1.0 m Projection*, based on post-AR4 results (raised cosine distribution with $\Delta z = 1.0$ m and $W/2 = 1.0$ m); key is right-hand column of dots in the bottom left-hand corner.

of multiplying factor coincide with *small* values of the scale parameter and *vice versa*.

For the world, the reciprocal of the scale parameter and its spatial variation are 10.2 ± 4.6 (sd) m^{-1}. The ± one standard deviation range yields a range of multiplying factor for 0.5 m sea-level rise of 16 to 1600.

Online Resource, Fig. (i), shows the same data, but restricted to the Australian continent. For Australia, the reciprocal of the scale parameter and its spatial variation are 9.8 ± 2.8 (sd) m^{-1}. The ± one standard deviation range yields a range of multiplying factors for 0.5 m sea-level rise of 33 to 540.

6.3 IPCC A1FI Projection

These results cover the period 1990-2100, and are based on the A1FI emission scenario and the *AR4-adjusted TAR projections* (normal probability distribution, with $\Delta z = 0.542$ m and $\sigma = 0.168$ m). The sea-level rise allowance is shown (using the *central key* in the figures) in Fig. 4 (for the world) and in Online Resource, Fig. (i) (for Australia).

For the world, the sea-level rise allowance and its spatial variation are 0.686 ± 0.064 (sd) m. The average allowance represents a 26% increase over the mean sea-level rise, 0.542 m.

For Australia, the sea-level rise allowance and its spatial variation are 0.681 ± 0.040 (sd) m. The average allowance again represents a 26% increase over the mean sea-level rise, 0.542 m.

6.4 1.0/1.0 m Projection

These results cover the 21st century and are based on post-AR4 results (raised-cosine probability distribution, with $\Delta z = 1.0$ m and $W/2 = 1.0$ m). The sea-level rise allowance is shown (using the *right-hand key* in the figures) in Fig. 4 (for the world) and in Online Resource, Fig. (i) (for Australia).

For the world, the sea-level rise allowance and its spatial variation are 1.440 ± 0.105 (sd) m. The average allowance represents a 44% increase over the mean sea-level rise of 1.0 m.

For Australia, the sea-level rise allowance and its spatial variation are 1.444 ± 0.073 (sd) m. The average allowance again represents a 44% increase over the mean sea-level rise of 1.0 m.

7 Summary

Climate change requires that designers, planners and policymakers make suitable allowances for future conditions. On the coast, new infrastructure needs to be built higher, and planning schemes and policies need to be adapted to account for the raised sea level. It was shown in Section 3 that, in cases in which extreme flooding events are modified by an *uncertain* change in mean sea level, it is preferable to base future allowances upon estimates of the *expected number of exceedances in a given period* rather than on the *exceedance probability*. An allowance based on exceedance probability would tend, in cases where the exceedance probability is relatively high (say, > 0.5), to significantly underestimate the number of exceedances.

In Section 4, a simple relationship was developed which defines a sea-level rise allowance which conserves the *expected number of exceedances* under conditions of uncertain sea-level rise. This allowance depends only on the projected rise in mean sea level and its uncertainty, and on the scale parameter of a Gumbel distribution fitted to the cumulative distribution function (it is assumed that the scale parameter does not change with a rise in sea level). An attractive feature of this allowance is that it does not require that the expected number of exceedances be prescribed; it is independent of the chosen level of precaution.

This allowance is always *greater* than the mean projection of sea-level rise, Δz, because the Gumbel distribution ($N = \exp((\mu - z)/\lambda)$) has a *positive* second derivative ($N/(\lambda^2)$) with respect to z (as is also the case with the more general GEV distribution when fitted to observed storm tides). If, instead, the distribution had a zero second derivative (i.e. with N varying linearly with z) then the allowance would be exactly Δz for any uncertainty distribution, P.

The technique has been demonstrated using a near-global database of sea-level records, and two possible projections of sea-level rise for the 21st century: one based on the TAR and AR4 of the IPCC (the *IPCC A1FI Projection*), and the other based on research since the AR4 (the *1.0/1.0 m Projection*). The *1.0/1.0 m Projection* is about twice as large, both in mean and standard deviation, as the *IPCC A1FI Projection*.

The global variation of the Gumbel scale parameter is illustrated by showing the expected increase in the number of flooding events for a 0.5 m sea-level rise (the world: Fig. 4 and Online Resource, Table (ii); and Australia: Online Resource, Fig. (i)). This multiplying factor covers a typical range of 16 to 1600.

The sea-level rise allowance (Fig. 4; Online Resource, Fig. (i) and Table (ii)) also shows a significant spatial variation (due to changes in the Gumbel scale parameter), even though the projections of sea-level rise and its uncertainty are assumed constant. The *IPCC A1FI Projection* yields allowances for 1990-2100 of 0.686 ± 0.064 (sd) m, while the *1.0/1.0 m Projection* yields allowances for the 21st century of 1.440 ± 0.105 (sd) m (covering the near-global data set).

In conclusion, allowances for future sea-level rise need to account for both the *statistics of the storm tide* and the *statistics of the sea-level rise projections*.

Acknowledgements This paper was supported by the Australian Government's Cooperative Research Centres Programme through the Antarctic Climate & Ecosystems Cooperative Research Centre. Sea-level data were supplied by European Sea-Level Service, Global Sea Level Observing System (GLOSS) Delayed Mode Centre, Helpdesk Water (Netherlands), Instituto Español de Oceanographia (Spain), Istituto Talassografico di Trieste (Italy), Marine Environmental Data Service (Canada), National Oceanography Centre Liverpool (UK), National Tidal Centre (Bureau of Meteorology, Australia), Norwegian Mapping Authority, Service Hydroographique et Océanographique de la Marine (France), Swedish Meteorological and Hydrological Institute and University of Hawaii Sea Level Centre (USA).

References

Bindoff N, Willebrand J, Artale V, Cazenave A, Gregory J, Gulev S, Hanawa K, Quéré CL, Levitus S, Nojiri Y, Shum C, Talley L, Unnikrishnan A (2007) Climate Change 2007: The Physical Science Basis. Contribution of Working Group I to the Fourth Assessment Report of the Intergovernmental Panel on Climate Change, Cambridge University Press, Cambridge, United Kingdom and New York, NY, USA, chap 5, pp 385–432

van den Brink H, Können G (2011) Estimating 10000-year return values from short time series. International Journal of Climatology 31:115–126, DOI 10.1002/joc.2047

Church J, White N (2011) Sea-level rise from the late 19th to the early 21st century. Surveys in Geophysics DOI 10.1007/s10712-011-9119-1, published online: 30 March 2011

Church J, Gregory J, Huybrechts P, Kuhn M, Lambeck K, Nhuan M, Qin D, Woodworth P (2001) Climate Change 2001: The Scientific Basis, Contribution of Working Group 1 to the Third Assessment Report of the Intergovernmental Panel on Climate Change, Cambridge University Press, Cambridge, United Kingdom and New York, NY, USA, chap 11, pp 639–693

Coles S (2001) An Introduction to Statistical Modeling of Extreme Values. Springer-Verlag, London, Berlin, Heidelberg

Hunter J (2010) Estimating sea-level extremes under conditions of uncertain sea-level rise. Climatic Change 99(3):331–350, DOI 10.1007/s10584-009-9671-6

Le Quéré C, Raupach M, Canadell J, Marland G, et al (2009) Trends in the sources and sinks of carbon dioxide. Nature Geoscience 2:831–836, DOI 10.1038/ngeo689

Meehl G, Stocker T, Collins W, Friedlingstein P, Gaye A, Gregory J, Kitoh A, Knutti R, Murphy J, Noda A, Raper S, Watterson I, Weaver A, Zhao ZC (2007) Climate Change 2007: The Physical Science Basis. Contribution of Working Group I to the Fourth Assessment Report of the Intergovernmental Panel on

Climate Change, Cambridge University Press, Cambridge, United Kingdom and New York, NY, USA, chap 10, pp 747–845

Menéndez M, Woodworth P (2010) Changes in extreme high water levels based on a quasi-global tide-gauge data set. Journal of Geophysical Research 115(C10011), DOI 10.1029/2009JC005997

Nicholls R, Marinova N, Lowe J, Brown S, Vellinga P, de Gusmão D, Hinkel J, Tol R (2011) Sea-level rise and its possible impacts given a 'beyond 4°C world' in the twenty-first century. Philosophical Transactions of the Royal Society A: Mathematical, Physical and Engineering Sciences 369:161–181, DOI 10.1098/rsta.2010.0291

Pfeffer W, Harper J, O'Neel S (2008) Kinematic constraints on glacier contributions to 21st-century sea-level rise. Science 321(5894):1340–1343, DOI 10.1126/science.1159099

Pugh D (1996) Tides, Surges and Mean Sea-Level. John Wiley & Sons, reprinted with corrections, http://eprints.soton.ac.uk/19157/01/sea-level.pdf, Chichester, New York, Brisbane, Toronto and Singapore

Pugh D (2004) Changing sea levels: effects of tides, weather, and climate. Cambridge University Press

R Development Core Team (2008) R: A Language and Environment for Statistical Computing. R Foundation for Statistical Computing, Vienna, Austria, URL http://www.R-project.org, ISBN 3-900051-07-0

Rahmstorf S, Cazenave A, Church J, Hansen J, Keeling R, Parker D, Somerville R (2007) Recent climate observations compared to projections. Science 316(5825):709, DOI 10.1126/science.1136843

Woodworth P, Blackman D (2004) Evidence for systematic changes in extreme high waters since the mid-1970s. Journal of Climate 17(6):1190–1197, DOI 10.1175/1520-0442(2004)017<1190:EFSCIE>2.0.CO;2

Electronic Supplementary Material

A simple technique for estimating an allowance for uncertain sea-level rise

Climatic Change

John Hunter, Antarctic Climate & Ecosystems Cooperative Research Centre, Hobart, Tasmania, Australia

john.hunter@utas.edu.au

A Derivation of Allowances

Eq. 7 of main paper is:

$$\begin{aligned} N_{ov} &= \int_{-\infty}^{\infty} P(z') \exp\left(\frac{\mu - z + \Delta z + z'}{\lambda}\right) dz' \\ &= N \exp\left(\left(\Delta z + \lambda \ln\left(\int_{-\infty}^{\infty} P(z') \exp\left(\frac{z'}{\lambda}\right) dz'\right)\right) \Big/ \lambda\right) \end{aligned} \quad \text{(i)}$$

which is here evaluated for three different probability distributions, $P(z')$:

Normal Distribution:

If $P(z')$ is a normal distribution of zero mean and standard deviation, σ, then

$$P(z') = \frac{1}{\sigma\sqrt{2\pi}} \exp\left(-\frac{(z')^2}{2\sigma^2}\right) \quad \text{(ii)}$$

and Eq. (i) becomes

$$N_{ov} = N \exp\left(\left(\Delta z + \frac{\sigma^2}{2\lambda}\right) \Big/ \lambda\right) \quad \text{(iii)}$$

in which z in the original Gumbel distribution (N in Eq. 6 in main paper) has been replaced by $z - \Delta z - \sigma^2/(2\lambda)$; the distribution has been shifted vertically by $\Delta z + \sigma^2/(2\lambda)$.

Boxcar Distribution:

If, $P(z')$ is a boxcar (uniform) distribution of zero mean and full-width, W (and therefore standard deviation, $\sigma = W/(2\sqrt{3})$), then

$$P(z') = \frac{1}{W} \quad \text{for} \quad -W/2 < z' < W/2 \quad \text{otherwise} \quad 0 \tag{iv}$$

and Eq. (i) becomes

$$\begin{aligned} N_{ov} &= N \exp\left(\left(\Delta z + \lambda \ln\left(\frac{2\lambda}{W}\sinh\left(\frac{W}{2\lambda}\right)\right)\right)\Big/\,\lambda\right) \\ &= N \exp\left(\left(\Delta z + \lambda \ln\left(\frac{\lambda}{\sigma\sqrt{3}}\sinh\left(\frac{\sigma\sqrt{3}}{\lambda}\right)\right)\right)\Big/\,\lambda\right) \end{aligned} \tag{v}$$

in which z in the original Gumbel distribution (N in Eq. 6 in main paper) has been replaced by $z - \Delta z - \lambda \ln(\cdots)$; the distribution has been shifted vertically by $\Delta z + \lambda \ln(\cdots)$.

Raised Cosine Distribution:

Finally, if $P(z')$ is a raised cosine distribution of zero mean and full-width, W (and therefore standard deviation, $\sigma = (W/2)\sqrt{1/3 - 2/(\pi^2)} = W/(2K)$ where $K = 1/\sqrt{1/3 - 2/(\pi^2)}$), then

$$P(z') = \frac{1}{W}\left(1 + \cos\left(\frac{2\pi z'}{W}\right)\right) \quad \text{for} \quad -W/2 < z' < W/2 \quad \text{otherwise} \quad 0 \tag{vi}$$

and Eq. (i) becomes

$$\begin{aligned} N_{ov} &= N \exp\left(\left(\Delta z + \lambda \ln\left(\frac{2\lambda}{W}\sinh\left(\frac{W}{2\lambda}\right)\left(\frac{(2\pi\lambda/W)^2}{1 + (2\pi\lambda/W)^2}\right)\right)\right)\Big/\,\lambda\right) \\ &= N \exp\left(\left(\Delta z + \lambda \ln\left(\frac{\lambda}{K\sigma}\sinh\left(\frac{K\sigma}{\lambda}\right)\left(\frac{(\pi\lambda/\sigma)^2}{K^2 + (\pi\lambda/\sigma)^2}\right)\right)\right)\Big/\,\lambda\right) \end{aligned} \tag{vii}$$

in which z in the original Gumbel distribution (N in Eq. 6 in main paper) has been replaced by $z - \Delta z - \lambda \ln(\cdots)$; the distribution has been shifted vertically by $\Delta z + \lambda \ln(\cdots)$.

Summary:

Therefore, the appropriate allowances (Z_n, Z_b and Z_r, for normal, boxcar and raised cosine distributions, respectively) for uncertain sea-level rise, which maintain the same expected number of flooding events in a given period, are

$$Z_n = \Delta z + \frac{\sigma^2}{2\lambda}$$
for a normal distribution, (viii)

$$\begin{aligned} Z_b &= \Delta z + \lambda \ln\left(\frac{2\lambda}{W}\sinh\left(\frac{W}{2\lambda}\right)\right) \\ &= \Delta z + \lambda \ln\left(\frac{\lambda}{\sigma\sqrt{3}}\sinh\left(\frac{\sigma\sqrt{3}}{\lambda}\right)\right) \end{aligned}$$
for a boxcar distribution, and (ix)

$$\begin{aligned} Z_r &= \Delta z + \lambda \ln\left(\frac{2\lambda}{W}\sinh\left(\frac{W}{2\lambda}\right)\left(\frac{(2\pi\lambda/W)^2}{1+(2\pi\lambda/W)^2}\right)\right) \\ &= \Delta z + \lambda \ln\left(\frac{\lambda}{K\sigma}\sinh\left(\frac{K\sigma}{\lambda}\right)\left(\frac{(\pi\lambda/\sigma)^2}{K^2+(\pi\lambda/\sigma)^2}\right)\right) \end{aligned}$$
for a raised cosine distribution (x)

It may be shown that $Z_n \geq Z_b$ and $Z_n \geq Z_r$ for all σ/λ. A conservative allowance for sea-level rise is therefore Z_n (Eq. (viii)). However, the raised cosine distribution (which yields the allowance given by Eq. (x)) is probably the more appropriate, given that there are physical constraints (and hence probable limits) on the rate of future sea-level rise (see Section 5.2 of main paper).

B The Uncertainty of the Projections

The derivation of the standard error of the best estimate of the projections from the results of the TAR (Third Assessment Report of the Intergovernmental Panel on Climate Change or IPCC) and AR4 (Fourth Assessment Report of the IPCC) is not straightforward. If the projections from individual models were independent, then it would only be necessary to estimate the number of degrees of freedom, n, and to calculate the standard error, σ, from the standard deviation, s, from

$$\sigma^2 = \frac{s^2}{n} \quad \text{(xi)}$$

The AR4 projections were based on 19 AOGCMs (Atmosphere-Ocean General Circulation Models), which were run on emission scenarios B1, A1B and A2. The remaining scenarios were modelled using the MAGICC (Model for the Assessment of Greenhouse-gas Induced

Climate Change) simple climate model (e.g. Meinshausen et al 2011), using empirical time-dependent ratios between pairs of scenarios (one of which was modelled using AOGCMs). It is tempting to assume that the models are independent and to associate the number of degrees of freedom, n, with the number of models used in the preparation of the AR4 projections (of order 20). However, Masson and Knutti (2011) performed a hierarchical clustering of the CMIP3 (phase 3 of the Coupled Model Intercomparison Project; the models reported in AR4) climate models and concluded that, due to widespread sharing of history, algorithms and components between models, 'the number of structurally different models is small', indicating that the actual number of degrees of freedom is significantly smaller than 20. Pennell and Reichler (2011) statistically analysed the results of 24 CMIP3 models and concluded that the effective number of models was only about 8. Furthermore, due to the strong interdependence of the models, it is likely that important aspects of the physics is either missing or wrong in *all models*, giving a bias which cannot be deduced from the scatter of model results, and which represents an *additional* uncertainty. Clear examples of this are the treatment of glaciers, ice caps and ice sheets (for which there is only *one* series of models contributing to the AR4 results) and the modelling of sulfate aerosols (a number of models sharing common observational data). Due to these considerations, the uncertainty, σ, is here associated with the *standard deviation* (rather than the *standard error*) of the projections.

C Initial Processing of the GESLA Sea-Level Database

The GESLA (Global Extreme Sea-Level Analysis) dataset was initially processed as follows:

1. only files which are at least 30 years in length (defined by the number of months containing at least some data, divided by 12) were selected,
2. non-physical outliers (identified as outliers which did not have any obvious cause, such as a tsunami or a tropical cyclone) and datum shifts (identified by a clear vertical offset, often bracketing a significant data gap) were addressed, either by removal or adjustment of data,
3. known tsunamis were removed,
4. where records were duplicated in separate files, the one which appeared most free of errors was selected, and
5. co-located data covering different time periods was joined, with appropriate adjustment for any datum shift.

This resulted in 198 records, of which 166 were unchanged from the original *GESLA* files, 28 were subject to some modification and 4 were the result of joining records. These records contain both tides and storm surges.

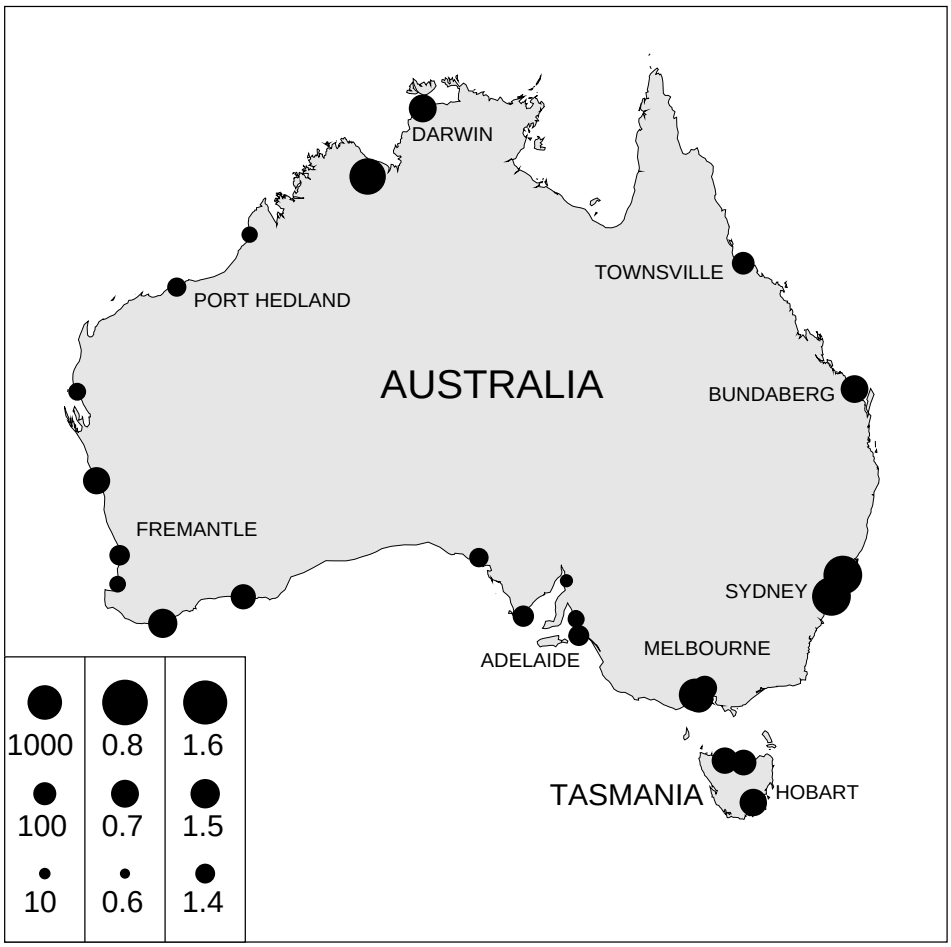

Figure (i): Results of Australian analysis, indicated by dot diameter. (a) Factor by which frequency of flooding events will increase with a rise in sea level of 0.5 metres (key is left-hand column of dots in the bottom left-hand corner). (b) Sea-level rise allowance (metres) for 1990-2100 which conserves frequency of flooding events for the *IPCC A1FI Projection* based on A1FI emission scenario and *AR4-adjusted TAR projections* (normal distribution with $\Delta z = 0.542$ m and $\sigma = 0.168$ m); key is central column of dots in the bottom left-hand corner. (c) Sea-level rise allowance (metres) for 21st century which conserves frequency of flooding events for the *1.0/1.0 m Projection*, based on post-AR4 results (raised cosine distribution with $\Delta z = 1.0$ m and $W/2 = 1.0$ m); key is right-hand column of dots in the bottom left-hand corner.

Table (i): Range of global sea-level rise from post-AR4 research (after Nicholls et al 2011). [a]Higher rates are possible for shorter periods. [b]For the twenty-first century. [c]For the best palaeo-temperature record.

Sea-level Rise (m century^{-1})	Methodological approach	Source
0.5-1.4	semi-empirical projection[b]	Rahmstorf 2007
0.8-2.4[a]	palaeo-climate analogue	Rohling et al 2008
0.55-1.10	synthesis[b]	Vellinga et al 2009
0.8-2.0	physical-constraint analysis[b]	Pfeffer et al 2008
0.56-0.92[a]	palaeo-climate analogue	Kopp et al 2009
0.75-1.90	semi-empirical projection[b]	Vermeer and Rahmstorf 2009
0.72-1.60[c]	semi-empirical projection[b]	Grinsted et al 2010

Table (ii): Summary of analyses for specific locations. [a]Large values such as this indicate that any locations which have been flooded in the past will be flooded on a daily basis with 0.5 m of sea-level rise (the ranges of sea-level variation at Cristóbal and Rikitea are only 0.6-0.9 m).

Location	Increase in frequency of flooding events for sea-level rise of 0.5 m	Sea-level rise allowance, 1990-2100, *IPCC A1FI Projection* (m)	Sea-level rise allowance, twenty-first century, *1.0/ 1.0 m Projection* (m)
Antofagasta (Chile)	9,000	0.800	1.608
Canary Islands (Spain)	571	0.722	1.521
Cape Town (South Africa)	12,600	0.809	1.616
Cristóbal (Panama)	465,000[a]	0.911	1.686
Fremantle (Australia)	61.2	0.659	1.409
Furuögrund (Sweden)	13.6	0.616	1.297
Honningsvåg (Norway)	74.6	0.664	1.421
Honolulu (USA)	6,010	0.788	1.597
Key West (USA)	5,970	0.788	1.597
Kwajalein (Marshall Islands)	15,100	0.814	1.621
La Coruña (Spain)	181	0.689	1.470
Nagasaki (Japan)	1,700	0.753	1.560
New York (USA)	22.3	0.630	1.338
Oslo (Norway)	18.0	0.624	1.321
Rikitea (French Polynesia)	147,000[a]	0.879	1.667
Rio de Janeiro (Brazil)	65.1	0.661	1.413
San Diego (USA)	3,160	0.770	1.579
Seattle (USA)	117	0.677	1.447
Sheerness (UK)	35.2	0.643	1.372
Sydney (Australia)	2,250	0.761	1.569
Trieste (Italy)	84.2	0.668	1.428
Wellington (New Zealand)	2,910	0.768	1.577

References

Grinsted A, Moore J, Jevrejeva S (2010) Reconstructing sea level from paleo and projected temperatures 200 to 2100 AD. Climate Dynamics 34:461–472, DOI 10.1007/s00382-008-0507-2

Kopp R, Simons F, Mitrovica J, Maloof A, Oppenheimer M (2009) Probabilistic assessment of sea level during the last interglacial stage. Nature 462:863–867, DOI 10.1038/nature08686

Masson D, Knutti R (2011) Climate model genealogy. Geophysical Research Letters 38(L08703), DOI 10.1029/2011GL046864

Meinshausen M, Raper S, Wigley T (2011) Emulating coupled atmosphere-ocean and carbon cycle models with a simpler model, MAGICC6 – Part 1: Model description and calibration. Atmospheric Chemistry and Physics 11:1417–1456, DOI 10.5194/acp-11-1417-2011

Nicholls R, Marinova N, Lowe J, Brown S, Vellinga P, de Gusmão D, Hinkel J, Tol R (2011) Sea-level rise and its possible impacts given a 'beyond 4°C world' in the twenty-first century. Philosophical Transactions of the Royal Society A: Mathematical, Physical and Engineering Sciences 369:161–181, DOI 10.1098/rsta.2010.0291

Pennell C, Reichler T (2011) On the effective number of climate models. Journal of Climate 24:2358–2367, DOI 10.1175/2010JCLI3814.1

Pfeffer W, Harper J, O'Neel S (2008) Kinematic constraints on glacier contributions to 21st-century sea-level rise. Science 321(5894):1340–1343, DOI 10.1126/science.1159099

Rahmstorf S (2007) A semi-empirical approach to projecting future sea-level rise. Science 315(5810):368–370, DOI 10.1126/science.1135456

Rohling E, Grant K, Hemleben C, Siddall M, Hoogakker B, Bolshaw M, Kucera M (2008) High rates of sea-level rise during the last interglacial period. Nature Geoscience 1:38–42, DOI 10.1038/ngeo.2007.28

Vellinga P, Katsman C, Sterl A, Beersma J, Hazeleger W, Church J, Kopp R, Kroon D, Oppenheimer M, Plag H, Rahmstorf S, Lowe J, Ridley J, von Storch H, Vaughan D, van de Wal R, Weisse R, Kwadijk J, Lammersen R, Marinova N (2009) Exploring high-end climate change scenarios for flood protection of the Netherlands. Tech. Rep. WR 2009-05, Wageningen University and Research Centre / Alterra and Royal Netherlands Meteorological Institute (KNMI)

Vermeer M, Rahmstorf S (2009) Global sea level linked to global temperature. Proceedings of the National Academy of Sciences 106(51):21,527–21,532, DOI 10.1073/pnas.0907765106